

Power System Node Loadability Evaluation Using Flexibility Analysis Method

W.Q. Sun¹, K. Xia¹, H.Y. Li¹, C.M. Wang²

¹Department of Electrical Engineering, University of Shanghai for Science & Technology, Jungong Rd. 516, Shanghai, China

²Department of Electrical Engineering, Shanghai Jiaotong University, Dongchuan Rd. 800, Shanghai, China
sidsqw@hotmail.com

Abstract—System transfer capability evaluation is an important research topic in power system analysis. However, as the uncertainty of load increasing direction, researches on the upper bound of system transfer capability appear to be too optimistic, whereas researches on the lower bound of system transfer capability appear to be too pessimistic. Actually, as load increasing direction cannot be forecasted accurately in practical power systems, obvious flaws in evaluating system transfer capability using deterministic analysis methods exist. In this paper, a method is proposed to give an approximate evaluation on power system node loadability using flexibility analysis method. Conventional rigid node voltage constraints are expressed into flexible form, and a set of critical node voltage values are obtained by solving a standard nonlinear optimization model using interior point algorithm. With the adjustment strategies given, such critical node voltage values show a strong positive correlation with the loadability on the corresponding nodes. Besides, compared with conventional methods, the method proposed can significantly improve the calculation efficiency for the same research purpose. Case study on IEEE 30-bus test system validates the effectiveness of the method proposed.

Index Terms—Flexibility analysis, load increasing, power system estimation, transfer capability.

I. INTRODUCTION

The notion of transfer capability is widely used in power system online dispatching as well as network planning. The computation results can give clear evidences for grid managers how many load margins the system remains. Existing researches mainly focus on system transfer capability within voltage stability constraints. And the research hotspots are the upper bound of system transfer capability (maximum transfer capability P_{Lmax}) as well as the lower bound of system transfer capability (min-max transfer capability $P_{Lmin-max}$ [1]).

A. Maximum Transfer Capability

Power system maximum transfer capability is investigated in two different ways.

One is that the load increasing direction is determined, namely load on each node increases on a same ratio at one

time. In such cases, the solution for maximum transfer capability is just the same as the solution for maximum load growth factor. In [2], interior point algorithm was used to determine the maximum transfer capability of a power system. In [3], ordinal optimization method was used to determine the best location of FACTS (flexible AC transmission system) to enhance transmission system transfer capability.

The other is to determine the optimal load increasing direction using optimization methods. On such an optimal load increasing direction, system transfer capability can be maximized within stability and safety constraints, so that the existing system can be fully used. In [4], the problem of total transfer capability evaluation was investigated using a probabilistic approach, and a nonlinear programming model for calculating transfer capability was presented.

In brief, load increasing directions are vested or optimized in maximum transfer capability researches. The results obtained are ideal situations which can hardly be fully realized in practical power system developments. Thus, such vested or optimized load increasing directions only have theoretical significances, but appear to be too optimistic in practical operations. For such reasons, a more conservative concept in power system transfer capability evaluation was proposed, namely the min-max transfer capability.

B. Min-Max Transfer Capability

Compared with maximum transfer capability analysis, power system min-max transfer capability evaluation tries to find out the lower bound of system transfer capability. In other words, min-max transfer capability researches focus on the worst load increasing direction, on which the maximum load increment is minimal. The main research difficulty is that such a min-max optimization problem is hard to solve using conventional optimization methods.

In [5], a method for calculating the distance from a point on the loadability surface to the closest point of nonsmoothness of the loadability surface was proposed. In [6], using two consecutive scalar local measurements, a simple local index for online estimation of closeness to loadability limit was introduced. In [7], using particle swarm optimization algorithm, the shortest distance from the operating point to the boundary of voltage stability was determined. In [8], a new

Manuscript received September 23, 2013; accepted February 6, 2014.

This research was funded by a grant (No. 14YF1410100) from "Yangfan Project" of Shanghai, China; and grants (No. 51177099 and 51207092) from the National Natural Science Foundation of China.

nodal loading model called “hyper-cone” model was proposed and the worst cases were defined and solved.

Compared with maximum load increment, min-max load increment is much more conservative, as such a min-max load increment can be realized on any load increasing direction without causing system instability or safety constraint violations. However, such an evaluation on system transfer capability is regarded as too pessimistic. And on such a load increasing direction, it is not conducive to make full use of power system resources.

Node loadability evaluation has a strong relationship with system transfer capability evaluation, as system load increment is the linear combination of single node load increment. But the calculation time will be huge if node loadability is evaluated one by one. It is eager that node loadability distribution can be given conveniently.

On the other hand, almost all the existing researches focus on the maximum or min-max power system transfer capability within system voltage stability constraints. But actually, most of the electrical equipment in power systems cannot work properly with a voltage lower than the lower voltage limit, which is usually higher than the voltage at collapse point. Such a problem was also realized in voltage stability index researches [9], where voltage limits, especially their lower limits were considered. Besides, other system operation constraints such as generator power output constraints and transmission line capacity constraints should also be taken into consideration in system transfer capability analysis.

Aiming at the disadvantages in conventional system transfer capability analysis, both P_{Lmax} and $P_{Lmin-max}$, the motivation of this paper is first introduced. Then, the basic principle, namely the relationship between node voltage and its loadability is elaborated. After that, conventional rigid node voltage constraints are expressed into flexible form, a system transfer capability estimation method using flexibility analysis is proposed, and the adjustment strategies are given. Finally, case study on IEEE 30-bus test system is made, and some conclusions are given.

II. MOTIVATION

From the introduction above, it can be found that both the upper bound and the lower bound of system transfer capability (P_{Lmax} and $P_{Lmin-max}$) are extreme cases in load increasing. Their numerical relationships in system transfer capability analysis are shown in Fig. 1.

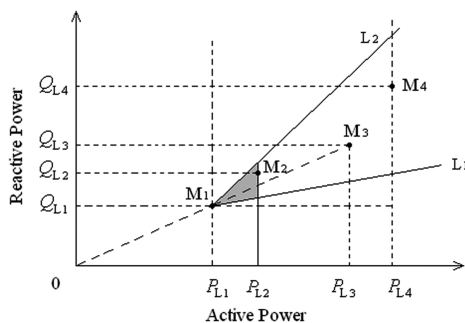


Fig. 1. Schematic diagram of system transfer capability.

In Fig. 1, point $M_1(P_{L1}, Q_{L1})$ refers to the current system operating point, where P_{L1}, Q_{L1} are the sums of system active

and reactive power loads respectively.

Assume that load on each node keeps a constant power factor when load increases, and then the system load increasing direction is constrained by the maximum and minimum load power factor angles among the nodes. Namely in Fig. 1, the angle α_{Lmin} between line L_1 and line $Q = Q_{L1}$, and the angle α_{Lmax} between line L_2 and line $Q = Q_{L1}$ can be obtained from (1) as follows:

$$\begin{cases} \alpha_{Lmin} = \min\{\alpha_{Li}\}, \\ \alpha_{Lmax} = \max\{\alpha_{Li}\}, \end{cases} \quad (1)$$

where α_{Li} is the load power factor angle of node i .

Thus, the possible system load increasing directions are between line L_1 and line L_2 .

Point $M_2(P_{L2}, Q_{L2})$ refers to the min-max system transfer capability point, where $P_{L2} = P_{L1} + P_{Lmin-max}$. Vector $\overline{M_1M_2}$ refers to the worst system load increasing direction. From the analysis above, it can be known that $P_{Lmin-max}$ refers to an arbitrary load increment that will not cause system instability or safety constraint violations. So the grey area surrounded by line L_1 , L_2 , and $P = P_{L2}$ is the absolute feasible system load increasing area.

Point $M_3(P_{L3}, Q_{L3})$ and $M_4(P_{L4}, Q_{L4})$ refer to the maximum load increment obtained by two different load increasing modes. Point M_3 corresponds to the load increasing mode in continuation power flow [10] (load on each node increases on a same ratio at one time), whereas point M_4 corresponds to the optimized load increasing direction. Vector $\overline{M_1M_4}$ refers to the most ideal system load increasing direction. Obviously, the numerical value among P_{L1} , P_{L2} , P_{L3} , and P_{L4} is $P_{L1} \leq P_{L2} \leq P_{L3} \leq P_{L4}$. And in many cases, $P_{L2} \ll P_{L4}$. In other words, there is huge difference in system transfer capability evaluation between the most ideal and the worst load increasing directions. Correspondingly, power system asset utilization can also be different in different load increasing modes.

The area surrounded by line L_1 , line L_2 , line $P = P_{L2}$, and line $P = P_{L4}$ is the possible feasible system load increasing area, where the feasibility depends on the load increasing directions (load increasing mode).

In practical power systems, power loads will increase along neither $\overline{M_1M_2}$ (worst direction) nor $\overline{M_1M_4}$ (optimal direction), as there exist huge amount of uncertainties in power load increasing. In Fig. 1, the absolute feasible system load increasing area is certain, but it is a pity that the system is much more likely to operate in the possible feasible system load increasing area when power load increases. Because such an area can access system load increment without increasing extra power equipment investments; thus, system equipment utilization can also be improved. As such an area is intension unclear and extension clear, the system transfer capability problem is actually a “grey” problem [11].

For the reasons above, existing power system transfer capability researches are theoretical researches focus on two

extreme cases. As for the “grey” area between the two extremes, it can hardly be described clearly.

III. NODE LOADABILITY EVALUATION

Node loadability analysis has a significant reference value to system transfer capability analysis. Thus, some analysis on a simplest 2-bus system as shown in Fig. 2 is first made.

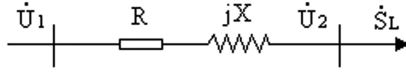


Fig. 2. A 2-bus system.

In Fig. 2, node voltage $\dot{U}_1 = U_1 \angle \delta_1$, $\dot{U}_2 = U_2 \angle \delta_2$; R, X are resistance and reactance of the transmission line respectively; $\dot{S}_L = S_L \angle \alpha_L = P_L + jQ_L$ is the load power. From KCL (Kirchhoff current law) and KVL (Kirchhoff voltage law), the relationship between \dot{U}_1, \dot{U}_2 can be formulated as follows

$$\dot{U}_2 = [U_1 - (P_L R + Q_L X) / U_1] - j[(P_L X - Q_L R) / U_1]. \quad (2)$$

As node voltage amplitude mainly depends on the real part of the voltage, an approximate equation can be obtained as follows as (3), from which it can be seen that the voltage drop is approximately proportional to $(R + X \tan \alpha_L)$ when load active power P_L is determined

$$\begin{aligned} \Delta U &= U_1 - U_2 \approx (P_L R + Q_L X) / U_1 = \\ &= P_L (R + X \tan \alpha_L) / U_1 \propto (R + X \tan \alpha_L). \end{aligned} \quad (3)$$

On the other hand, if U_1 is determined, the node loadability on node 2 considering lower limit of U_2 can be approximately expressed as (4)

$$U_2 \approx [U_1 - (P_L R + Q_L X) / U_1] \geq U_{2\min}. \quad (4)$$

Then the limit of node loadability can be obtained as (5)

$$P_L \leq U_1 (U_1 - U_{2\min}) / (R + X \tan \alpha_L). \quad (5)$$

From (5), it can be seen that the maximum node loadability is approximately proportional to $(R + X \tan \alpha_L)^{-1}$; in other words, inverse proportional to $(R + X \tan \alpha_L)$. And from (3) and (5), it can be concluded that, when regarding node voltage limit as the main factor that affects node loadability, the node voltage drop at current node load power can reflect the potential node loadability to some extent.

However, practical power systems cannot be as simple as the system above. There may be more than one transmission path for a load, and power load on one node may receive different amount of power quantities from different power resources according to grid dispatching modes. In such situations, it is doubtful that whether node voltage amplitude can still reflect the node loadability.

For a certain power system with determined power loads and operation constraints, the maximum transfer capability on one node is also determined on condition that generation

power output adjustment is considered. But node voltage amplitude at current system load distribution can be different in different grid dispatching modes. Some measures must be taken to guarantee the uniqueness of node voltage amplitude if it is attempted to be used as the estimation evidence of node loadability evaluation.

In complex power systems, power transfers from power resources to loads through power transmission network. If power load only increases on a single node and its node voltage lower limit is regarded as the main factor that hinders the load increasing, situation may be that load increases until the node voltage reaches its lower limit. Situations may be similar on other nodes when single node loadability is analysed on them.

Since single node loadability has a great relationship with the voltage drop when the power is transferred from power resources to load through the transmission network, what will happen if the upper voltage limits of the whole system are artificially reduced to a critical level? Results may be that voltage level of the whole system becomes lower with the reduction of upper voltage limits until voltage on one or some load nodes reach their lower limits.

There are reasons to believe that, compared with load nodes with comparatively higher voltages, load nodes with comparatively lower voltages in such a situation remains less node loadability. Due to the grid structure and load distribution, more voltage drop has been consumed on these nodes than on other nodes. So the critical node voltage amplitude distribution of load nodes at this time may give evidences on the approximate evaluation of transfer capability on each node.

IV. METHODS AND PROBLEM FORMULATION

In this section, conventional rigid node voltage constraints are first expressed into flexible forms and system voltage flexibility index is defined. Then, a standard nonlinear optimization model is established to solve the system operation state with a lowest voltage level. Finally, some adjustment measures are taken to make the estimation evidences more accurate.

A. Flexible Expression of Node Voltage Constraints

Node voltage constraint is one of the most important as well as the most widely considered safety constraints in power system analysis and optimization. Node voltage constraints in power system analysis are usually expressed as (6) in rigid form as follows

$$U_{i\min} \leq U_i \leq U_{i\max}, \quad (6)$$

where $U_{i\min}, U_{i\max}$ are the lower and upper voltage limits of node i respectively.

From (6), it can be seen that both the upper and lower limits of node voltage constraints are artificially set and their values are fixed. In other words, they are rigid constraints with not any flexibility.

As it is introduced above, the upper limits of node voltage constraints are considered to be artificially reduced to find a critical system operation state with a lowest voltage level.

Node voltage constraints are then expressed into flexible form in (7) as follows

$$U_{i\min} \leq U_i \leq U_{i\max} - u_i \Delta U_i, \quad (7)$$

where ΔU_i is the variation of the upper voltage limit of node i , and u_i is its variation factor.

If ΔU_i in each flexible node voltage constraint is valued as shown in (8), the value range of u_i is $u_i \in [0,1]$

$$\Delta U_i = U_{i\max} - U_{i\min}. \quad (8)$$

From (7) and (8), it can be seen that $u_i = 0$ corresponds to the largest voltage constraint domain, whereas $u_i = 1$ corresponds to the smallest domain. So u_i can be regarded as the node voltage flexibility index of node i .

From the method above, conventional rigid node voltage constraints are transformed into flexible forms, and the critical system operation state desired can be obtained from a standard nonlinear optimization model as follows.

B. Solution Model of Critical System Voltage Level

Assume that u_i is equal for each node, namely $u_i = u$, then a system operation state with critical node voltage level can be obtained by solving the optimization model (9) as follows:

$$\begin{aligned} & \max u \\ & \text{s.t.} \begin{cases} P_{Gi} + P_i(u, x) = P_{Li}, \\ Q_{Gi} + Q_i(u, x) = Q_{Li}, \\ P_{Gi\min} \leq P_{Gi} \leq P_{Gi\max}, \\ Q_{Gi\min} \leq Q_{Gi} \leq Q_{Gi\max}, \\ U_{i\min} \leq U_i \leq U_{i\max} - u \cdot \Delta U_i, \\ S_{l\min} \leq S_l \leq S_{l\max}, \\ i = 1, 2, \dots, n, \quad l = 1, 2, \dots, L, \end{cases} \end{aligned} \quad (9)$$

where u, x refer to the vectors of control and state variables respectively; equality constraints are node active and reactive power balance respectively; inequality constraints are generator active and reactive power output constraints, flexible node voltage constraints, and transmission line capacity constraints respectively; n, L are the total node and transmission line number of the system respectively.

In model (9), the upper voltage limit of each node is reduced on a same ratio. With such a reduction, a unique critical node voltage amplitude distribution can be obtained when u is maximized within the constraints.

In the power flow results obtained, system power loads are transferred in a way that the overall system voltage loss is minimized. So the critical node voltages obtained roughly reflect the comprehensive node voltage loss level of its power receiving channels.

Optimization model (9) is a standard multi-dimensional nonlinear programming problem. Interior point algorithm [12] is used to solve it in this paper.

C. Adjustment Strategies

In the section above, node voltage constraint is regarded as the most important factor that affects node loadability. But as model (9) described, there are other constraints such as generator power output constraints and transmission line capacity constraints in practical power system analysis, which may also affect the results of node loadability analysis.

Thus, adjustments to the critical node voltage values obtained from model (9) according to generator power output distribution and transmission line power flow distribution are necessary to make the results more suitable for node loadability distribution estimation.

The adjustment objects are load nodes directly connected with generators or load nodes connected with generators through a node without loads; besides, the power flow direction must be from generators to the nodes. Such load nodes will be called as "related load nodes" in the adjustment strategies introduction as follows.

The adjustment strategies proposed follow the three rules as follows.

1. *Rule 1:* if both the generator and the transmission path remain margins, replace the node voltage of the related load node with the generator node voltage;
2. *Rule 2:* if either the generator or the transmission line remains little or no margins, take no adjustments on the related load nodes;
3. *Rule 3:* if the related load node acts as both load node and intermediate node (or generator node), take flexible adjustments according to the power flow results.

V. CASE STUDY

IEEE 30-bus test system [13] is taken as the case study in this paper. It contains 24 PQ nodes, 5 PV nodes, and 1 V node. Base value of the per-unit system is $S_B = 100$ MVA, $U_B = 135$ KV. Assume that the voltage limits are as follows:

$$\begin{cases} U_{i\min} = 0.95\text{p.u.}, & \text{for all nodes,} \\ U_{i\max} = 1.05\text{p.u.}, & \text{for PQ nodes,} \\ U_{i\max} = 1.10\text{p.u.}, & \text{for PV and V}\theta \text{ nodes.} \end{cases} \quad (10)$$

The system connection diagram is shown as Fig. 3.

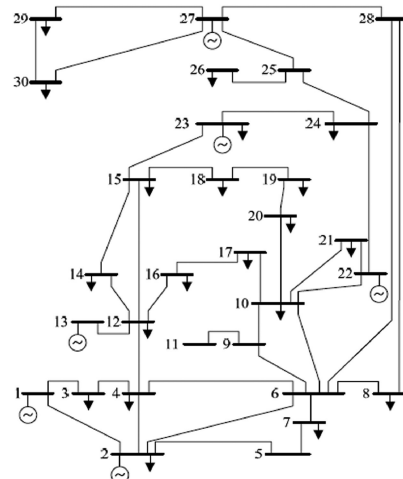


Fig. 3. Diagram of IEEE 30-bus test system.

System operation state with critical node voltage distribution is obtained by solving model (9). The critical situation appears when $u = 0.509$, and the node voltages obtained are listed with per-unit values in Table I.

TABLE I. CRITICAL NODE VOLTAGES.

i	Type	U_i	i	Type	U_i	i	Type	U_i
1	V	1.011	11	PQ	0.991	21	PQ	0.999
2	PV	1.017	12	PQ	0.997	22	PV	1.006
3	PQ	0.999	13	PV	1.024	23	PV	0.993
4	PQ	0.997	14	PQ	0.985	24	PQ	0.992
5	PQ	0.999	15	PQ	0.986	25	PQ	0.999
6	PQ	0.990	16	PQ	0.987	26	PQ	0.981
7	PQ	0.985	17	PQ	0.984	27	PV	1.012
8	PQ	0.950	18	PQ	0.975	28	PQ	0.987
9	PQ	0.991	19	PQ	0.972	29	PQ	0.992
10	PQ	0.991	20	PQ	0.976	30	PQ	0.981

And the generator power outputs and their limits are listed with per-unit values in Table II.

TABLE II. GENERATOR POWER OUTPUTS AND THEIR LIMITS.

No.(i)	P_{Gi}	Q_{Gi}	$P_{Gi \min}$	$P_{Gi \max}$	$Q_{Gi \min}$	$Q_{Gi \max}$
1	0.444	-0.191	0	0.800	-0.200	1.500
2	0.137	0.577	0	0.450	-0.200	0.600
13	0.400	0.203	0	0.400	-0.150	0.447
22	0.260	0.383	0	0.500	-0.150	0.625
23	0.284	-0.060	0	0.300	-0.100	0.400
27	0.400	0.120	0	0.400	-0.150	0.487

On the other hand, single node loadability is evaluated one by one. The optimization results for each node are listed with per-unit values in Table III. Node loadability for nodes those have not loads in initial state is not considered.

TABLE III. NODE LOADABILITY FOR EACH NODE.

No.(i)	Load Increment	No.(i)	Load Increment	No.(i)	Load Increment
1	/	11	/	21	0.345+j0.221
2	0.894+j0.514	12	0.726+j0.486	22	/
3	0.873+j0.437	13	/	23	0.582+j0.291
4	0.880+j0.185	14	0.359+j0.093	24	0.244+j0.188
5	/	15	0.446+j0.136	25	/
6	/	16	0.374+j0.192	26	0.090+j0.059
7	0.843+j0.403	17	0.304+j0.196	27	/
8	0.115+j0.115	18	0.219+j0.062	28	/
9	/	19	0.261+j0.093	29	0.119+j0.045
10	0.620+j0.214	20	0.288+j0.092	30	0.133+j0.024

From Table III, it can be seen that there are 20 nodes with loads in initial state, namely node 2, 3, 4, 7, 8, 10, 12, 14 to 21, 22, 23, 25, 28, and 29. The power factors of the increased loads are just the same as their initial loads.

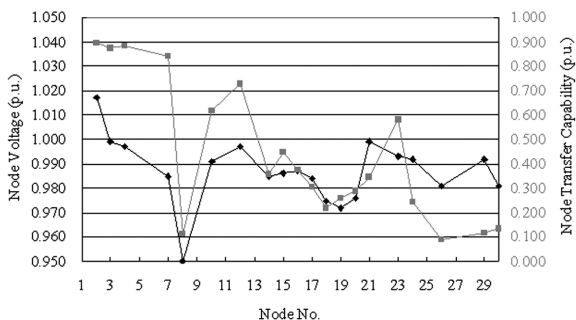


Fig. 4. Schematic comparison between critical node voltage distribution and node loadability distribution.

Compare the maximum transfer capability (active power) of each node with the corresponding node voltages listed in Table I; the schematic comparison is shown as Fig. 4. The black line refers to node voltage distribution, and it corresponds to the left vertical axis; the grey line refers to single node loadability distribution, and it corresponds to the right vertical axis.

In Fig. 4, there appears an intuitive correlation between the two series. Regression analysis tools in MS Excel 2003 are used to make mathematical analysis.

Regression analysis results show that the correlation coefficient is 0.6515, which corresponds to a moderately strong positive correlation [14]. And the probability of type 1 error (Significance F) is 0.00186, which means the confidence of the model is greater than 99.8 %.

System transfer capability is then calculated, the optimal result obtained is $\Delta S_{L \max} = 1.069 + j0.615$ p.u., and the corresponding load increment on each node is $\Delta S_{L2} = 0.631 + j0.369$ p.u., $\Delta S_{L23} = 0.243 + j0.121$ p.u., $\Delta S_{L24} = 0.130 + j0.100$ p.u., $\Delta S_{L29} = 0.066 + j0.025$ p.u.

From such a result, it can be seen that single node loadability analysis is significant basis of system transfer capability analysis, as node 2 and 23 undertake more than 80 % of the active power load increment when system maximum transfer capability is considered.

Then adjustment measures are taken according to the strategies proposed. The adjustment measures are listed in Table IV.

TABLE IV. ADJUSTMENT STRATEGIES.

Gen. No.	$P_{Gi} / P_{Gi \max}$	Generator margin	Related load nodes	Adjustment strategies
1	0.44/0.80	adequate	2, 3	$U_2 = \max\{U_1, U_2\}$, $U_3 = U_1$
2	0.14/0.45	adequate	4, 7, 8	$U_4 = U_2, U_7 = U_2$
13	0.40/0.40	none	12	$U_{12} = U_{13}$
22	0.26/0.50	adequate	10, 21	$U_{10} = U_{22}$
23	0.28/0.30	little	15, 24	no adjustments
27	0.40/0.40	none	6, 8, 24, 26, 29, 30	no adjustments

Comments for the adjustment measures:

- Node 2 is a load node as well as a generator node, and it is linked with generator node 1, so U_2 is replaced with the greater one between U_1 and U_2 , namely $U_2 = \max\{U_1, U_2\}$ (Rule 1 & 3);
- Node 8 is not adjusted as line 6-8 undertaking a heavy load $S_{6-8} = 0.1588 + j0.1704$ p.u., which is near its upper limit $|S_{6-8}|_{\max} = 0.32$ p.u. (Rule 2);
- Node 12 is adjusted although generator node 13 remains no active power margins, as most of the active power generated by generator 13 in such a situation are transferred to other loads through node 12. When load increases on node 12, generator 13 can undertake the load increment and the power vacancy can be filled by other generators (Rule 3);
- Node 21 is not adjusted as line 22-21 undertaking a

heavy load $S_{22-21} = 0.2525 + j0.1965$ p.u.,
 $|S_{22-21}| = 0.32\text{p.u.} = |S_{22-21}|_{\max}$ (Rule 2);
 5. Node 15 and 24 are not adjusted as line 23-15 undertaking a heavy load $S_{23-15} = 0.1554 - j0.0383$ p.u.,
 $|S_{23-15}| = 0.16\text{p.u.} = |S_{23-15}|_{\max}$; meanwhile, generator 23 remains little active power margins (Rule 2);
 6. Node 6, 8, 24, 26, 29, and 30 are not adjusted as generator node 27 is the only power resource at that area, and it remains no active power margins (Rule 2);
 7. Other node voltages are adjusted according to Rule 1.
 Schematic comparison between adjusted node voltage and node loadability is shown in Fig. 5.

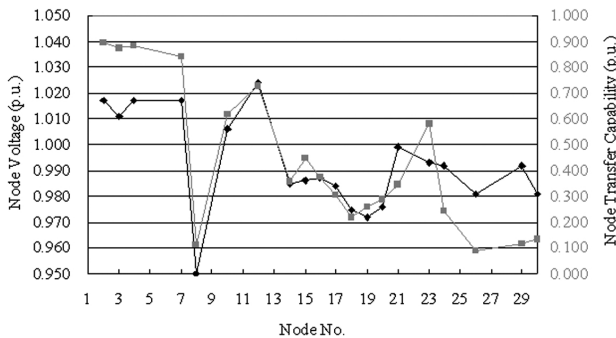


Fig. 5. Schematic comparison between adjusted critical node voltage distribution and node loadability distribution.

From Fig. 5, it can be seen that there appears a much stronger positive correlation between the two series. Regression analysis shows that the correlation coefficient is 0.8493, and the probability of type 1 error is 2.174×10^{-6} at this time. In other words, there exists a quite strong positive correlation between the two series, and the confidence of the model is now greater than 99.999 %.

A more detailed regression analysis result about the estimation accuracy is compared in Table V.

TABLE V. COMPARISON OF ESTIMATION ACCURACY.

Regression analysis index	Before adjustment	After adjustment
Correlation Coefficient	0.65146	0.84930
Determination Coefficient	0.42440	0.72131
Adjusted Determination Coefficient	0.39242	0.70583
Standard Error	0.01049	0.01013
Residual Error	0.00198	0.00185
Significance F	0.00186	2.174×10^{-6}

From Table V, it can be seen that there appears a stronger positive correlation after the adjust measures, which shows that the adjust measures are effective.

VI. CONCLUSIONS

System transfer capability analysis is an attractive reach topic in power system evaluation. Existing methods are deterministic methods, which try to find out the optimal or the worst load increasing directions. And system voltage collapse is usually used as the limit criterion. There are two main flaws in such analysis methods as they are analysed in the paper. Besides, other system safety constraints such as generator power output limits and transmission line capacity limits can also make significant effects on system transfer capability, so they should also be taken into consideration in system transfer

capability evaluation.

Considering that node voltage loss is the main factor that hinders node loadability, node voltage constraints are first transferred from conventional rigid form into flexible form. And the upper limits of node voltages are continually reduced until a critical system voltage level appears. Such a critical node voltage distribution show moderately strong positive correlation with single node loadability. Then, some adjustment measures are taken to the critical node voltage values according to the situation of other system operation constraints. After that, the correlation becomes much stronger.

Compared with the one by one node loadability calculation in a power system with n_l load nodes, the method proposed can save as much as about $(n_l-1)/n_l$ calculation times in evaluating node loadability distribution. Further researches may focus on how to further improve the estimation accuracy.

REFERENCES

- [1] D. Q. Gan, X. C. Luo, D. V. Bourcier, R. J. Thomas, "Min-max transfer capabilities of transmission interfaces", *Int. Journal of Electrical Power & Energy Systems*, vol. 25, no. 5, pp. 347–353, 2003. [Online]. Available: [http://dx.doi.org/10.1016/S0142-0615\(02\)00099-6](http://dx.doi.org/10.1016/S0142-0615(02)00099-6)
- [2] Y. Dai, J. D. McCalley, V. Vittal, "Simplification, expansion and enhancement of direct interior point algorithm for power system maximum loadability", *IEEE Trans. Power Systems*, 2002, vol. 15, no. 3, pp. 1014–1021.
- [3] Y. C. Chang, R. F. Chang, T. Y. Hsiao, C. N. Lu, "Transmission system loadability enhancement study by ordinal optimization method", *IEEE Trans. Power Systems*, vol. 6, no. 1, pp. 451–459, 2011. [Online]. Available: <http://dx.doi.org/10.1109/TPWRS.2010.2049667>
- [4] W. X. Li, P. Wang, Z. Z. Guo, "Determination of optimal total transfer capability using a probabilistic approach", *IEEE Trans. Power Systems*, vol. 21, no. 2, pp. 862–868, 2006. [Online]. Available: <http://dx.doi.org/10.1109/TPWRS.2006.873106>
- [5] M. Perninge, L. Soder, "On the validity of local approximations of the power system loadability surface", *IEEE Trans. Power Systems*, vol. 26, no. 4, pp. 2143–2153, 2011. [Online]. Available: <http://dx.doi.org/10.1109/TPWRS.2011.2115259>
- [6] M. Parniani, M. Vanouni, "A fast local index for online estimation of closeness to loadability limit", *IEEE Trans. Power Systems*, vol. 25, no. 1, pp. 584–585, 2010. [Online]. Available: <http://dx.doi.org/10.1109/TPWRS.2009.2036460>
- [7] M. J. Chen, B. Wu, C. Chen, "Determination of shortest distance to voltage instability with particle swarm optimization algorithm", *Eur. Trans. Elect. Power*, vol. 19, no. 8, pp. 1109–1117, 2009. [Online]. Available: <http://dx.doi.org/10.1002/etep.286>
- [8] Y. Kataoka, "A probabilistic nodal loading model and worst case solutions for electric power system voltage stability assessment", *IEEE Trans. Power Systems*, vol. 18, no. 4, pp. 1507–1514, 2003. [Online]. Available: <http://dx.doi.org/10.1109/TPWRS.2003.818691>
- [9] Y. Kataoka, M. Watanabe, S. Iwamoto, "A new voltage stability index considering voltage limits", in *Proc. Power Systems Conf. and Exposition, (PSCE 2006)*, 2006, pp. 1878–1883.
- [10] M. A. Kamarposhti, H. Lesani, "Contingencies ranking for voltage stability analysis using continuation power flow method", *Elektronika ir Elektrotechnika*, vol. 3, no. 99, pp. 73–76, 2010.
- [11] S. F. Liu, J. Forrest, Y. J. Yang, "A summary of the progress in grey system research", *IEEE Int. Conf. Grey Systems and Intelligent Services*, pp. 1–10, 2013.
- [12] N. Duvvuru, K. S. Swarup, "A hybrid interior point assisted differential evolution algorithm for economic dispatch", *IEEE Trans. Power Systems*, vol. 26, no. 2, pp. 541–549, 2011. [Online]. Available: <http://dx.doi.org/10.1109/TPWRS.2010.2053224>
- [13] A MATLAB power system simulation package, R. D. Zimmerman, C. E. Murillo-Sanchez, D. Gan. [Online]. Available: <http://www.pserc.cornell.edu/matpower/>
- [14] E. Viau, J. Peccia, "Survey of wastewater indicators and human pathogen genomes in biosolids produced by class A and class B stabilization treatments", *Applied and Environmental Microbiology*, vol. 75, no. 1, pp. 164–174, 2008. [Online]. Available: <http://dx.doi.org/10.1128/AEM.01331-08>